Artificial Intelligence in Agriculture 6 (2022) 34–46

Contents lists available at ScienceDirect

Artificial Intelligence in Agriculture

journal homepage: http://www.keaipublishing.com/en/journals/artificial-intelligence-in-agriculture/

Land suitability analysis for maize production using geospatial technologies in the Didessa watershed, Ethiopia

Mitiku Badasa Moisa [a,*], Firdissa Sadeta Tiye [b], Indale Niguse Dejene [c], Dessalegn Obsi Gemeda [d]

[a] Department of Agricultural Engineering, Faculty of Technology, Wollega University, Shambu Campus, Ethiopia
[b] Department of Geography and Environmental Studies, College of Social Sciences and Humanities, Wollega University, Gimbi Campus, Ethiopia
[c] Department of Earth Sciences, College of Natural and Computational Sciences, Wollega University, Nekemte Campus, Ethiopia
[d] Department of Natural Resources Management, College of Agriculture and Veterinary Medicine, Jimma University, Jimma, Ethiopia

ARTICLE INFO

Article history:
Received 22 December 2021
Received in revised form 3 February 2022
Accepted 8 February 2022
Available online 11 February 2022

Keywords:
Agricultural production
LULC
Land suitability
Overlay analysis
Pairwise comparison

ABSTRACT

Physical land suitability assessment is a prerequisite for enhancing yield production and enables the agricultural communities to use the right place for the right crops. Maize is one of stable one food crops of Ethiopia and cultivated in three agroecological zones: highland, midland and lowlands. Despite these facts, maize yield is very low due to a lack of knowledge and information gaps on land suitability. Physical land suitability for maize cultivation is essential to minimize the problem of food security. The present study aims to identify the potential land suitability for maize production in the Didessa watershed, Western Ethiopia using Multi-Criteria Evaluation (MCE) and geospatial technologies. Land use land cover (LULC) change, climate, topography, soil, and infrastructure facilities were considered for maize land suitability assessment. The MCE based pairwise comparison matrix was applied to estimate land suitability for maize crop cultivation. The results showed that, about 977.7 km^2 (14.1%) is highly suitable, 4794.9 km^2(69.1%) is moderately suitable while 1118.8 km^2 (16.1%), and 51.5 km^2 (0.7%) of the study area were categorized under marginally and not suitable for maize production, respectively. This research provides crucial information for decision making organs and the farming community to utilize potential areas for maize cultivation.

1. Introduction

At global level about 1, 162 million tons of maize are produced in 2020 (Solanki et al., 2020). Maize production in the world increased from 313 million tonnes in 1971 to 1162 million tonnes in 2020, which indicates an increment by 3.07% per year (Nyagumbo et al., 2016). Agriculture is the backbone and the major source of income in Ethiopia (Berhanu and Poulton, 2014; Headey et al., 2014). Maize farming is widely practiced in many regions of Ethiopia (Kassie et al., 2015). It is widely cultivated for commercial benefit not only in Ethiopia, but also at global level (Linda et al., 2015; Habibie et al., 2019). Despite this, some people are unable to eat because of a lack of food (Regassa and Stoecker, 2012; Mota et al., 2019). In poor nations such as Ethiopia, the inability to exploit existing technologies for yield development results in low maize yield (Asfaw et al., 2012; Abate et al., 2019). Low yield harvesting is results in food shortage caused by a lack of technological access have been reported in the country (Bewket, 2007; Dijk et al., 2020).

Around the late 17th century, maize crops were introduced in Ethiopia (Huffnagel, 1961; Abate et al., 2015). In Ethiopia, maize is cultivated in highland, midland, and lowland agro-ecological zones (Elias et al., 2013; Tessema and Simane, 2019; Dendir and Simane, 2019).

Increasing agricultural output through the use of innovative crop types and farm inputs in Ethiopia is gaining traction (Tamene et al., 2017; Sime and Aune, 2018; Silva et al., 2021). Apart from using better varieties and agricultural inputs, determining the appropriateness of a given parcel of land before investing in agriculture can help maximize the use of existing land resources (Ahamed et al., 2016). Land suitability assessment is very crucial for land use planning (Vasu et al., 2018; Habibie et al., 2019; Mehrjardi et al., 2020; Al-Taani et al., 2021). Despite its relevance, land suitability evaluation for maize production has received little attention in the country as a whole and in the study area specifically. In Ethiopia, some research has been conducted on the physical suitability of land for maize production (Girma et al., 2015; Alemu and Worku, 2017; Debesa et al., 2020). Biophysical parameters such as

Abbreviations: AEZ, Agro ecological zone; AHP, Analytical Hierarchy Process; CI, Consistency Index; CR, Consistency Ratio; DN, Digital number; IDW, Inverse Distance Weighting; LST, Land Surface Temperature; LULC, Land use land cover; MCE, Multi-Criteria Evaluation; MoWIE, Ministry of Water Irrigation Engineering; NDVI, Normalized Difference Vegetation Index; NMA, National Meteorological Agencies; USGS, U.S Geological Survey.

* Corresponding author.
E-mail address: mitikubadasa10@gmail.com (M.B. Moisa).

https://doi.org/10.1016/j.aiia.2022.02.001
2589-7217/

climate (rainfall and temperature), soil, land use, and elevation were included in prior studies. However, the land surface temperature (LST) was not considered in physical land suitability assessment in the previous research. Thus, this research intended to incorporate the LST as a physical land suitability determining criterion.

2. Materials and methods

2.1. Descriptions of the study area

This study was conducted in Didessa watershed in western parts of Ethiopia. Geographically, Didessa watershed is located between 7°49′30″ to 8°54′30"N and 36°1′00″ to 37°6′00″E (Fig. 1). The topography of the Didessa watershed ranges from 1354 m to 3154 m above mean sea level. The watershed covers a total area of 6942.9 km^2.

2.1.1. Climate

The study area received maximum amount rainfall during the summer season (June to September). Study conducted by Wedajo et al. (2019) in Didessa River sub basin indicates that the average minimum and maximum temperature is 13 °C, and 26.5 °C, respectively. Other study by Gemeda et al. (2021) at Bedele station, which is located within the Didessa River sub-basin found that the mean minimum and maximum temperature is about 11.9 °C, and 26.2 °C, respectively.

2.1.2. Soil types

The study area has a large variety of soil types. Among the existing soil types, Haplic Alisols was the most dominat which covers an area of 4235.7 km^2 (61.0%) and the least dominated soil type was Rhodic Nitisol with an area of 518.6 km^2 (7.5%).

2.2. Data sources and descriptions

Landsat images of OLI/TIRS 2020 were downloaded from U.S. Geological Survey (USGS) website (https://www.usgs.gov/) for Land use land cover (LULC) classification. Climate data was obtained from National Meteorological Agencies (NMA) of Ethiopia while soil data was obtained from Ministry of Water and Irrigation Engineering (MoWIE) and elevation data was extracted from ASTER DEM (Table 1; Fig. 2).

2.3. Data analysis

2.3.1. Rainfall

Rainfall data of four stations from near and within Didessa watershed namely Gimbi, Nekemte, Bedele and Arjo were obtained from

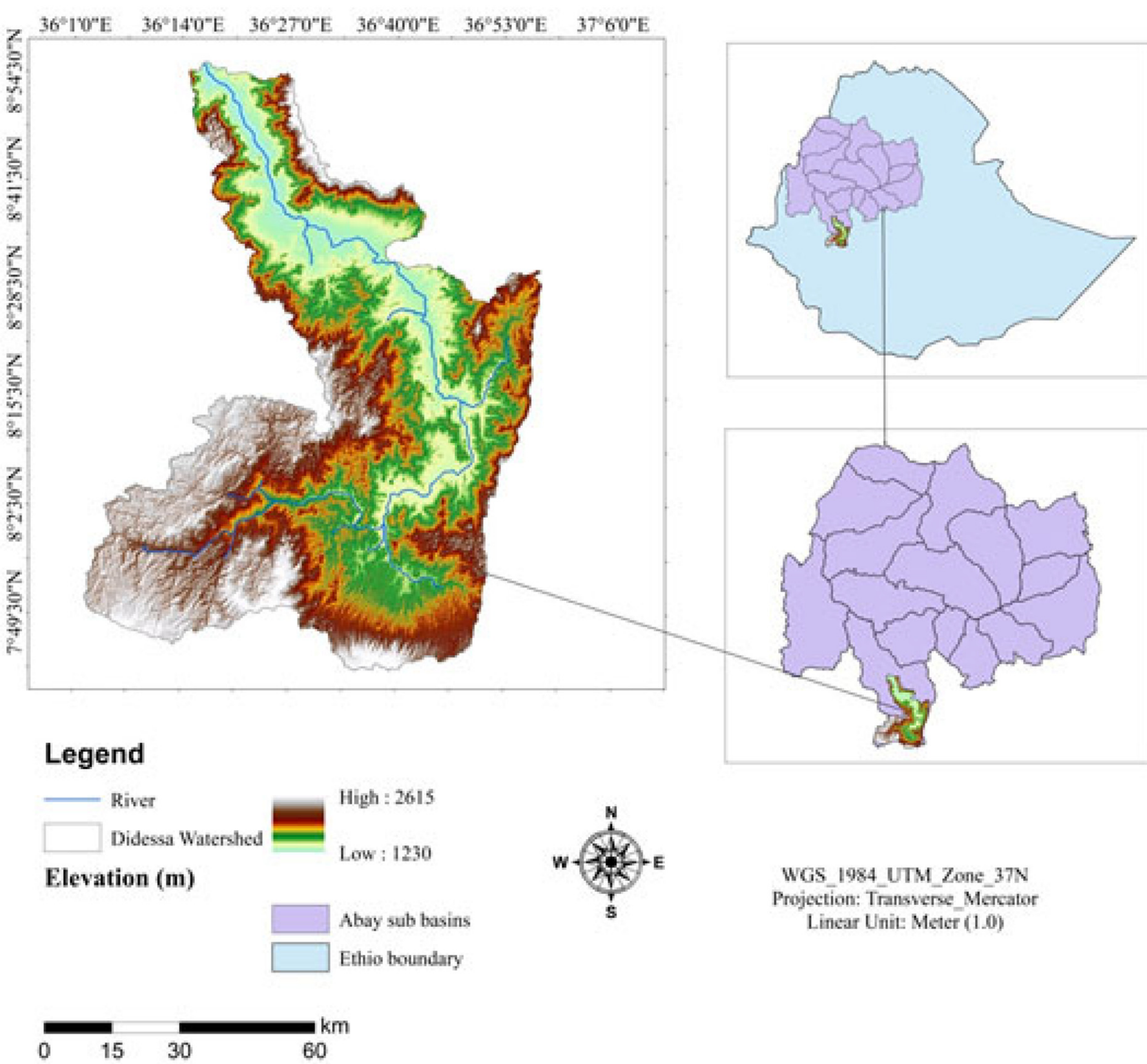

Fig. 1. Location map of the study area.

Table 1
Descriptions of data used for the study.

Data	Data types	Resolution(m)	Sources
Climate data	Rainfall data	30	NMA
Landsat OLI/TIRS	LST, LULC	30	USGS
ASTER DEM	Altitude	30	USGS
Soil data	Soil types, drainage, depth, and texture	30	MoWIE

Ethiopian National Meteorological Agency. We interpolated the climate data of four stations using Inverse Distance Weighting (IDW) techniques to obtain annual rainfall data for areas using stations in and around the study area. This annual rainfall was interpolated with a 30 m resolution and then extracted to the study area.

2.3.2. Land surface temperature

In the present study, the LST was retrieved from the thermal bands of the Landsat OLI/TIRS of 2020 (Adeola et al., 2017). The mono window algorithm was applied to retrieve LST from the thermal bands of the OLI/TIRS images. Accordingly, LST was retrieved from Landsat 8 (OLI/TIRS) with thermal bands of band 10 used by mono-window algorithm following (Guo et al., 2020; Sekertekin and Bonafoni, 2020). Digital number (DN) was converted to the spectral radiance of thermal bands of Landsat TIRS (Dener and Alves, 2016; Ziaul and Pal, 2018). Consequently, LST was estimated using the brightness temperature of the two bands of thermal infrared, mean and difference in land surface emissivity (Cheng et al., 2015).

Step 1: Conversion of digital numbers to top of atmosphere (TOA) spectral radiance

Thermal data in the Landsat sensor and deliver a manner of signifying pixels are stored in a digital number that has not yet been calibrated and converted into radiance units (Aik et al., 2020; Moisa et al., 2022) using (Eq. (1)).

$$L\lambda = (ML * QCal) + AL \quad (1)$$

where

$$L\lambda = Top\ of\ Atmosphere\ (TOA) spectral\ radiance\ \left(Wm^{-2}sr^{-1}\mu m^{-1}\right)$$

$$ML = Band-specific\ multiplicative\ rescaling\ factor\ from\ the\ metadata$$
$$(Radianne-multi-band\ x, where\ x\ is\ the\ band\ number$$

$$AL = Band-specific\ additive\ rescaling\ factor\ from\ the\ meta\ data$$
$$(Radiance-add-band\ x, where\ x\ is\ the\ band\ number$$

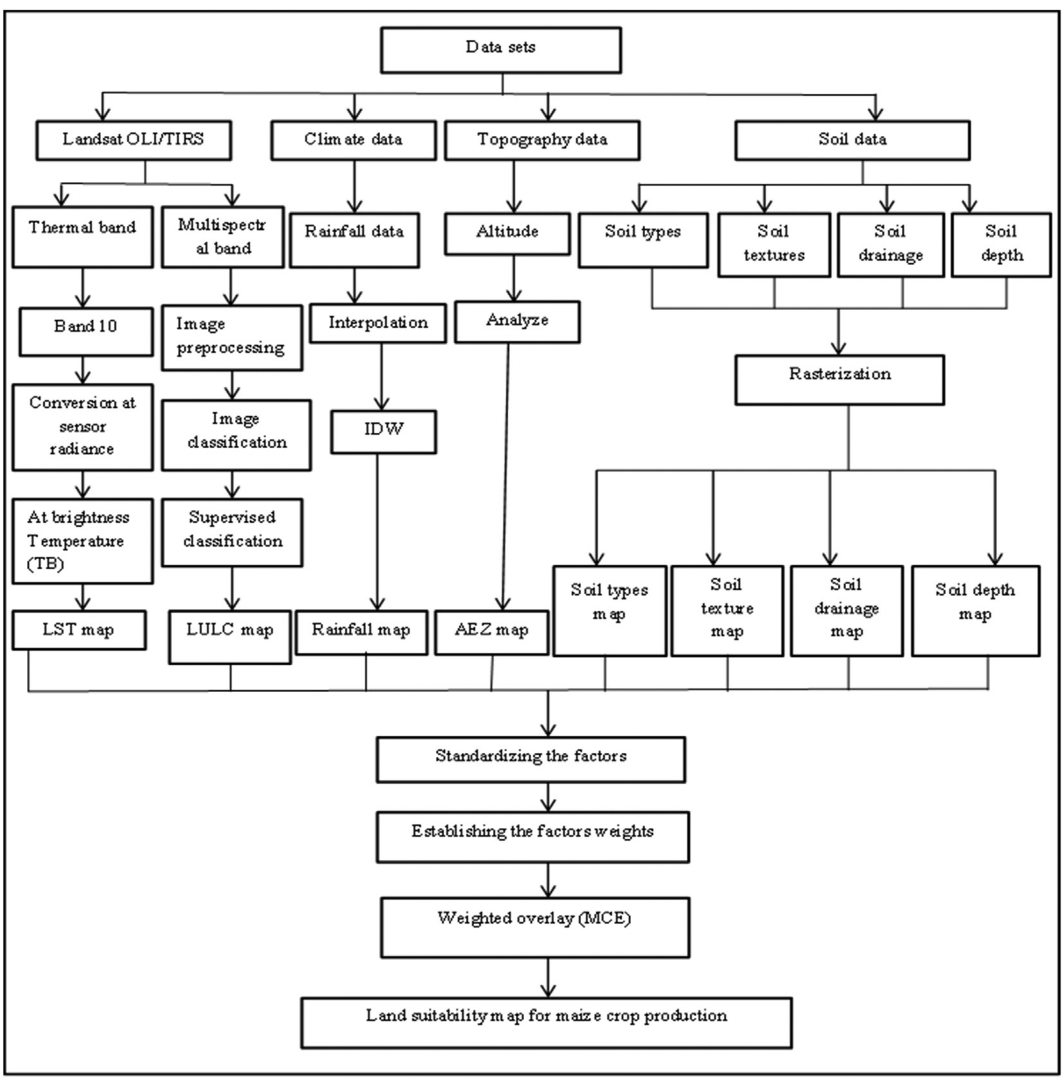

Fig. 2. Methodological flowchart of the study.

Table 2
Pairwise comparison matrix of parameters selected for this study.

Factors	Texture	Drainage	Soil types	LULC	Soil depth	Elevation	Rainfall	LST
Soil texture	1	2	2	2	2	3	3	4
Drainage	½	1	2	2	2	3	3	4
Soil Types	½	1/2	1	2	2	2	3	3
LULC	½	1/2	1/2	1	2	2	3	3
Soil depth	½	1/2	1/2	1/2	1	2	2	3
Elevation	1/3	1/3	1/2	1/2	1/2	1	2	3
Rainfall	1/3	1/3	1/3	1/3	1/2	1/2	1	2
LST	¼	1/4	1/3	1/3	1/3	1/3	1/2	1
Σ=	4.42	7.07	8.95	10.5	11.98	15.56	19.36	22.16

$Q\ Cal = Quantized\ and\ calibrated\ standard\ product\ pixel\ values\ (DN)$

Step 2: Conversion of radiance to brightness temperature

After the DNs are converted to radiance, the thermal band's spectral radiance should be converted to brightness temperature (BT) as recently used by Moisa et al. (2022) using (Eq. (2)).

$$\mathbf{BT} = \frac{\boldsymbol{K2}}{\boldsymbol{ln}\left(\frac{\boldsymbol{K1}}{\boldsymbol{L\lambda}} + \mathbf{1}\right)} \tag{2}$$

$BT = is\ effective\ at-sensor\ brightness\ temperature\ (K)$

$K2 = is\ calibration\ constant\ 2$

$K1 = is\ calibration\ constant\ 1$

$L\lambda = is\ the\ spectral\ radiance\ at\ the\ sensor'sapertune\ \left(\frac{W}{m^2 * sr * \mu m}\right);\ and$

$Ln = is\ natural\ logarithm$

Step 3: Land surface emissivity estimation using NDVI

The normalized difference vegetation index (NDVI) was utilized to classify the distributions of vegetation cover as well as their greenness. As a result, as a viable basis function, it investigates the transformation of NDVI into values related to the cover part by utilizing empirical correlations with vegetation indices (Tomar et al., 2013). NDVI calculation is critical for determining the proportion of vegetation (PV). Furthermore, emissivity (ε), which is linked to PV, should be determined (Eq. (3)).

$$NDVI = \frac{NIR - R}{NIR + R} \tag{3}$$

where

$NDVI = is\ the\ normalized\ difference\ vegetation\ index$

$NIR = is\ the\ near\ infrared\ band\ and\ R\ is\ the\ red\ band$

Landsat 8 uses Band 5 (Infrared) and 4 (Red) to estimate the NDVI values. After NDVI estimated, the proportion of vegetation was calculated, which indicates the land surface emissivity.

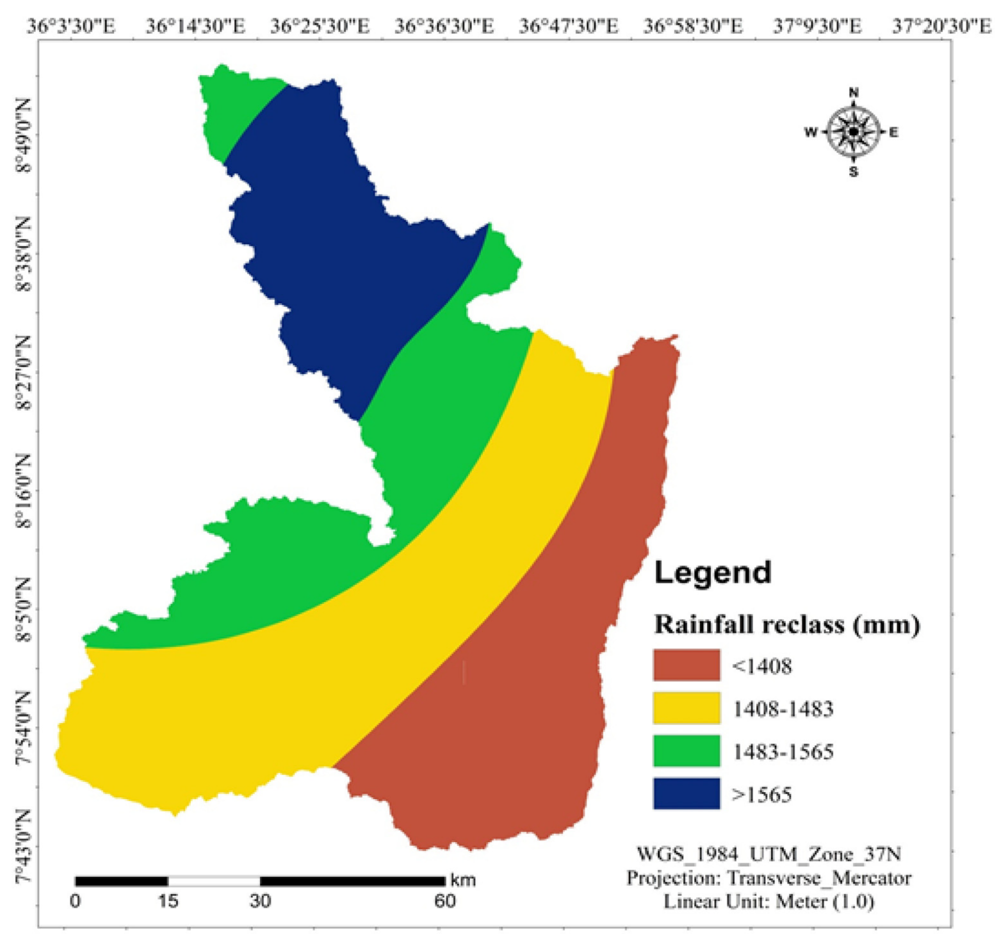

Fig. 3. Annual rainfall map of the study area.

Step 4: Estimating the proportion of vegetation

The proportion of vegetation was estimated using (Eq. (4)).

$$PV = \left(\frac{NDVI - NDVImin}{NDVImax - NDVImin}\right)2 \tag{4}$$

Step 5: Land surface emissivity

The land surface emissivity (ε) is significant for LST estimation. The land surface emissivity was calculated following (Sobrino et al., 2004; Chibuike et al., 2018) using (Eq. (5)).

$$\varepsilon = 0.004 * PV + 0.986 \tag{5}$$

The radiant surface temperature was corrected for emissivity using Eq. (6).

$$LST = \frac{TB}{1 + \left(\lambda \frac{TB}{P}\right) In\varepsilon} - 273.15 \tag{6}$$

where

LST = is land surface temperature (in Kelvin)

TB = is the radiant surface temperature (in Kelvin)

λ = is the wavelength of emitted radiance (11.5 μm)

$p = h * \frac{c}{\sigma(1.438 * 10^{-2}\ mk)}$; *h is Planck'sconstant* $(6.26 * 10^{-34}\ J\ S)$; *c* is the *velocity of light* $(2.998 * 10^{8}$ m/s); σ is the Stefan Boltzmann constant $(1.38^{*}\ 10^{-23}$ J $K^{-1})$; and ε is the land surface emissivity.

2.3.3. Elevation

The ASTER DEM with 30 m resolution downloaded from USGS website (https://www.usgs.gov/) and used to obtain the altitude (meter). From this organization we extract the topography of the study area, which very crucial to understand land suitability for maize production. Maize crop cultivation was more favorable in lowland areas and vice versa (Gorfu and Ahmed, 2011; Rashid et al., 2013).

2.3.4. Soil data

Soil data of the study area was obtained from the Ministry of Water and Irrigation Engineering and clipped to the study area. In addition, the soil data were converted to raster format by 30 m spatial resolution and reclassified according to a previous study Debesa et al. (2020) for overlay analysis.

2.3.5. Land use land cover types

Multispectral Landsat OLI/TIRS layer were stacked and extracted to the Didessa watershed. The LULC of the study area was classified using supervised classification maximum likelihood algorithm. An image was classified into cultivated land, forest, grassland, dense and open woodlands and urban areas using the ERDAS Imagine 2015 software.

2.4. Pairwise comparison approach for criteria weight estimation

Based on expert opinion weight values from comparison of the criteria were processed using the analytical hierarchy process (AHP) model (Saaty, 2004; Abine, 2021). This model was developed by Saaty (1980) to compare the relative importance of each criterion. Saaty (1980) provided the scale range to indicate the relative importance of

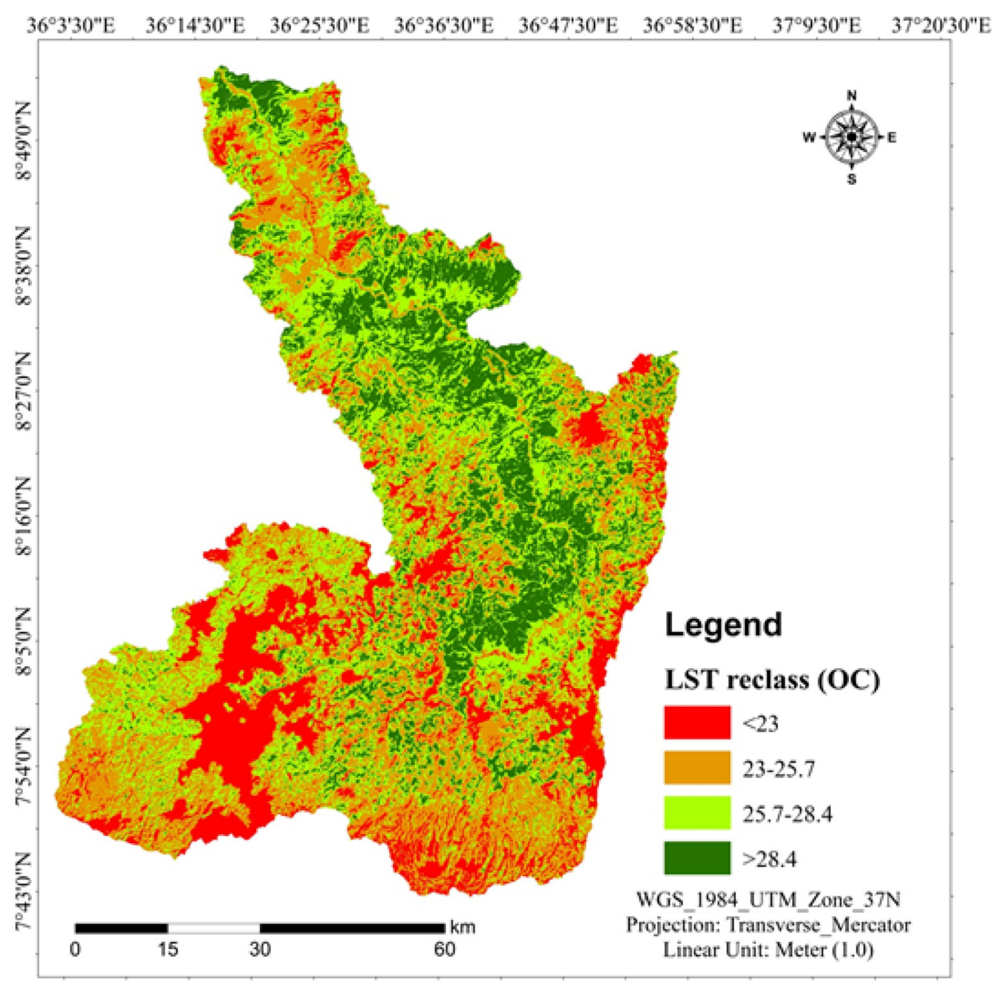

Fig. 4. Land surface temperature of the study area.

Table 3
LST classes and corresponding suitability classes.

S/No	LST classes (°C)	Area (km^2)	Area (%)	Suitability classes
1	<23	1171.3	16.9	Not suitable
2	23–25.7	2286.6	32.9	Marginally suitable
3	25.7–28.4	2144.7	30.9	Moderately suitable
4	>28.4	1340.3	19.3	Highly suitable
	Total	6942.9	100.0	

each factor, which ranges between one and nine. Finally, the weights of the pairwise comparison matrix priorities were computed (Table 2).

The consistency ratio (CR) was calculated to check the consistency of comparisons (Yohannes and Soromessa, 2018). The CR was calculated using (Eq. (7)). The CR values ranges from 0 to 1 (Saaty, 1980; Malczewski, 2000). A CR <0.1 is a reasonable level of consistency. Calculating consistency index (CI) is very important for crop land suitability analysis and calculated using Eq. (7).

$$CI = \frac{\lambda max - n}{n-1} \tag{7}$$

where λ max*is the largest eigenvalue of the pairwise comparision matrix and n is the number of classes*.

Then, CR is obtained using Eq. (8) as suggested by Saaty (1980).

$$CR = \frac{CI}{RI} \tag{8}$$

where RI id the ratio index over average value of CI for random metrices using the Saaty scale

Table 4
Agro-ecological zones and suitability classes of the study area.

S·N	Agro ecological zone	Area (km^2)	Area (%)	Suitability classes
1	Lowlands	1640.8	23.6	Highly suitable
2	Midlands	4990.8	71.9	Moderately suitable
3	Highlands	311.3	4.5	Marginally suitable
	Total	6942.9	100.0	

2.5. Weighted overlay analysis

All reclassified factors were aggregated and weighted using the function of overlay analysis in ArcGIS environment. A serious of pairwise comparison matrices application was performed to analyze the relative importance of all factors to be considered for land maize land suitability analysis as used by Debesa et al. (2020). The pairwise matrix comparison (Rabia and Terribile, 2013) were used using Eq. (9).

$$S = \Sigma WiXi \tag{9}$$

where S is suitability, Wi is weight of factor, and Xi is criterion score of factor i.

3. Results and discussion

3.1. Annual rainfall

Rainfall data were used to analyze the annual rainfall of the study area, which is one of the basic requirements for maize production. With-

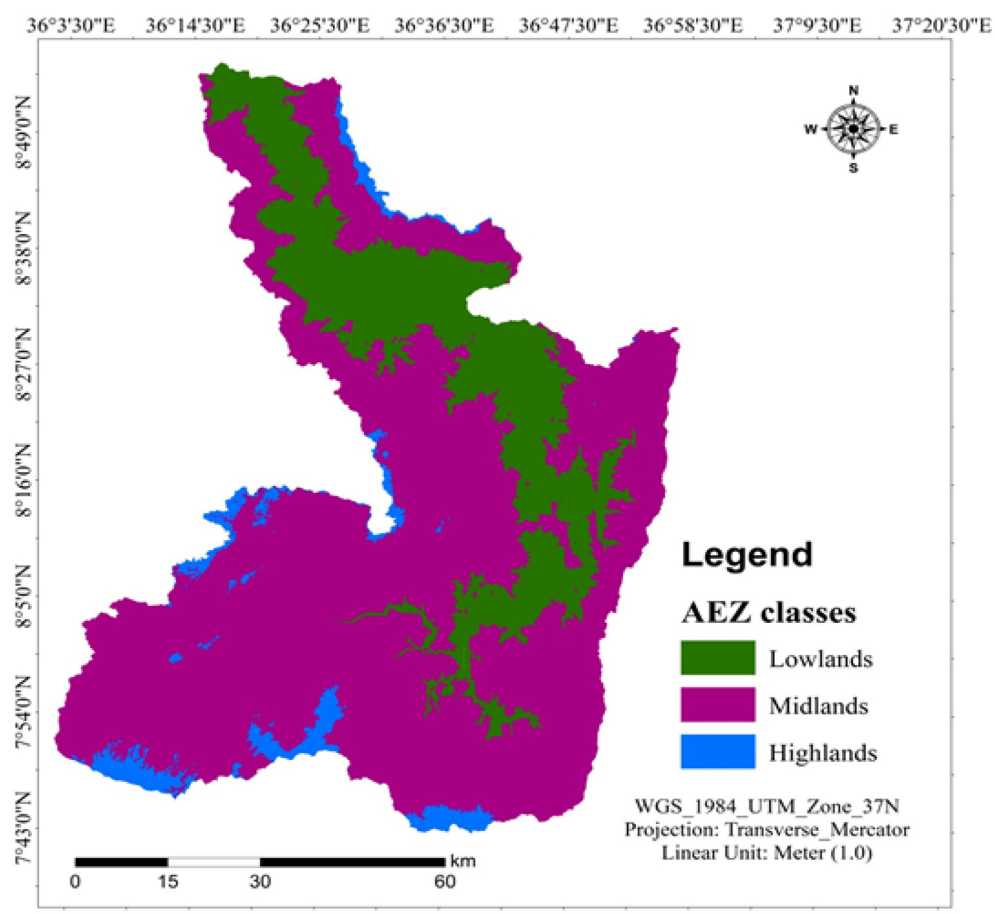

Fig. 5. Agro-ecological zone of the study area.

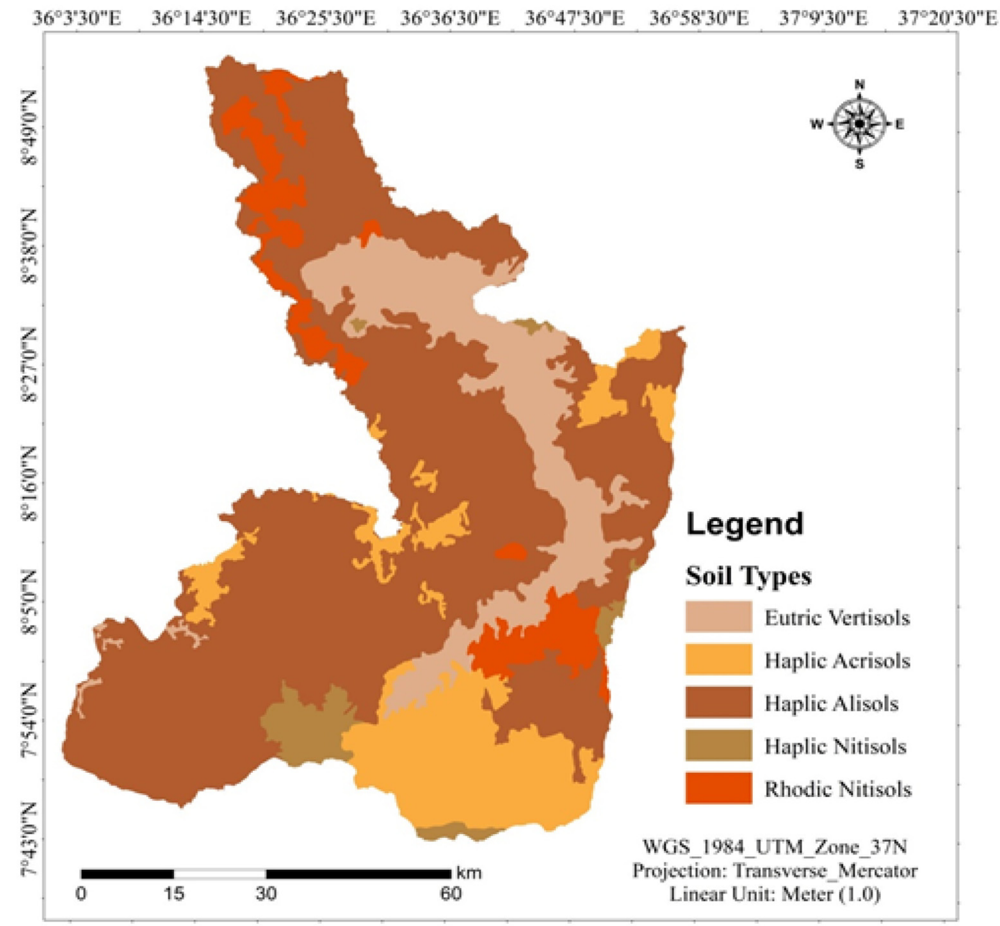

Fig. 6. Soil types of the study area.

out rainfall there is no agriculture specifically the rain-fed agriculture is not operational at all. The Didessa watershed's northwestern areas were unsuitable for maize crop development (Fig. 3). According to Kindu et al. (2009) stated that rainfall is most important parameter for site selection of maize crop cultivation.

3.2. Land surface temperature estimation

The LST of the study area was determined using the thermal band of OLI/TIRS 2020 Landsat image. Warm temperatures are suitable for maize crop cultivation, while cold temperatures are not. About 1340.3 km^2 (19.3%) of the study area is very appropriate for maize production. The most appropriate areas were concentrated in the central and northern parts of the study area (Fig. 4). However, with an area of 1171.3 km^2 (16.9%), the south western areas of the study area were not appropriate for maize crop production (Table 3). These findings are consistent with Habibie et al. (2019), who found that high LST are optimal for maize crop productivity.

Table 5
Soil types and their corresponding suitability classes.

S·N	Soil types	Area (km^2)	Area (%)	Suitability classes
1	Eutric Vertisols	988.2	14.2	Not suitable
2	Haplic Acrisols	991.2	14.3	Marginally suitable
3	Haplic Alisols	4235.7	61.0	Moderately suitable
4	Haplic Nitisols	209.1	3.0	Highly suitable
5	Rhodic Nitisols	518.6	7.5	Highly suitable
	Total	6942.9	100.0	

Table 6
Soil texture and their corresponding suitability classes of the study area.

S/No	Soil texture	Area (km^2)	Area (%)	Suitability classes
1	sandy clay	10.3	0.8	Not suitable
2	clay loam	127.5	1.8	Marginally suitable
3	sandy clay loam	3826.7	55.1	Moderately suitable
4	loam	80.7	1.2	Highly suitable
5	sandy loam	2478.0	35.0	Moderately suitable
6	loamy sand	419.8	6.0	Marginally suitable
	Total	6942.9	100.0	

3.3. Agro ecological zones of the study area

The agro-ecological zones of the study area were extracted from digital elevation model. Previous research Hurni (1998), Gorfu and Ahmed's (2011) were used to create the Agro ecological zone (AEZ) Didessa watershed. The findings of this study revealed that lowlands dominated core parts of the study area, whereas midlands dominated substantial portions (Fig. 5). Our results showed that a total of 1640.8 km^2 (23.6%) of the research area was found to be highly favorable for maize crop cultivation (Table 4). Previous studies conducted by Gorfu and Ahmed (2011) and Rashid et al. (2013) conclude that lowland areas are appropriate for maize farming.

3.4. Soil types

Eutric Vertisols, Haplic Acrisols, Haplic Alisols, Haplic Nitisols, and Rhodic Nitisols are among the major soil types in the study area (Fig. 6). Haplic nitisols and rhodic nitisols were found to be highly favorable for maize production, with an area of 727.7km^2 (10.5%) (Table 5). However, with a total area of 988.2km^2, Eutric vertisols were not

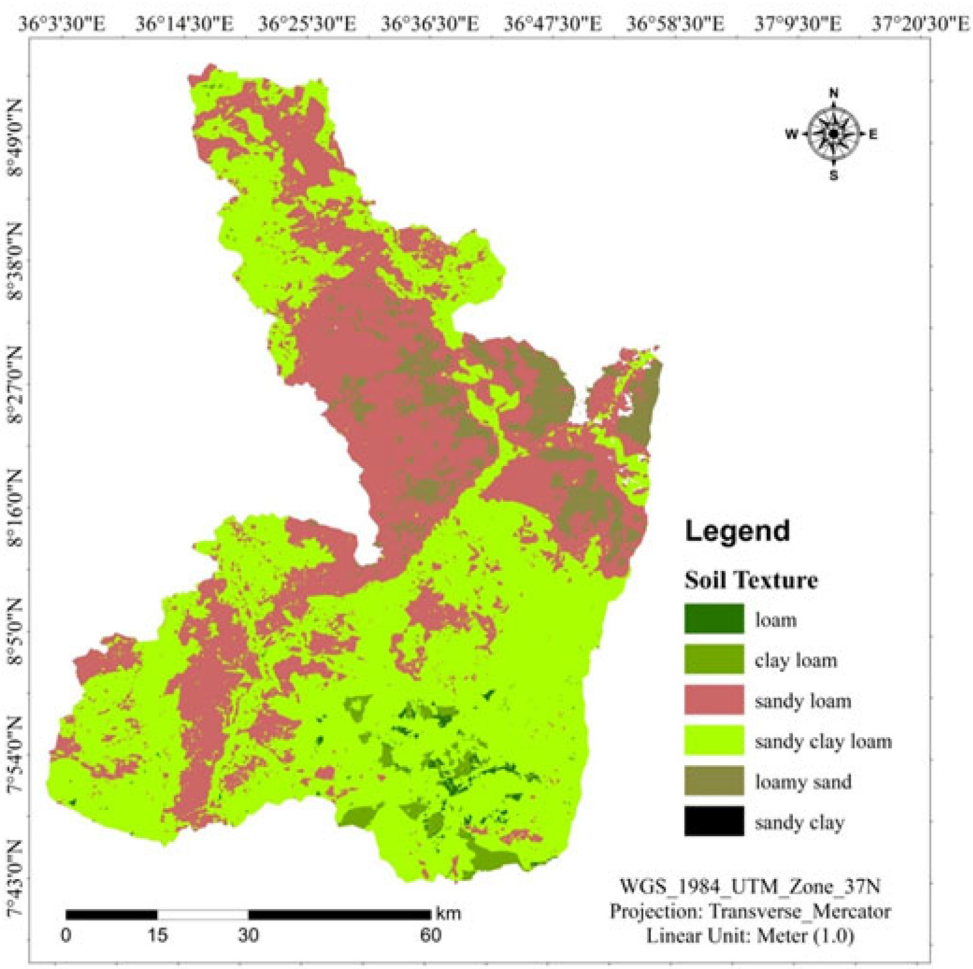

Fig. 7. Soil texture map of the study area.

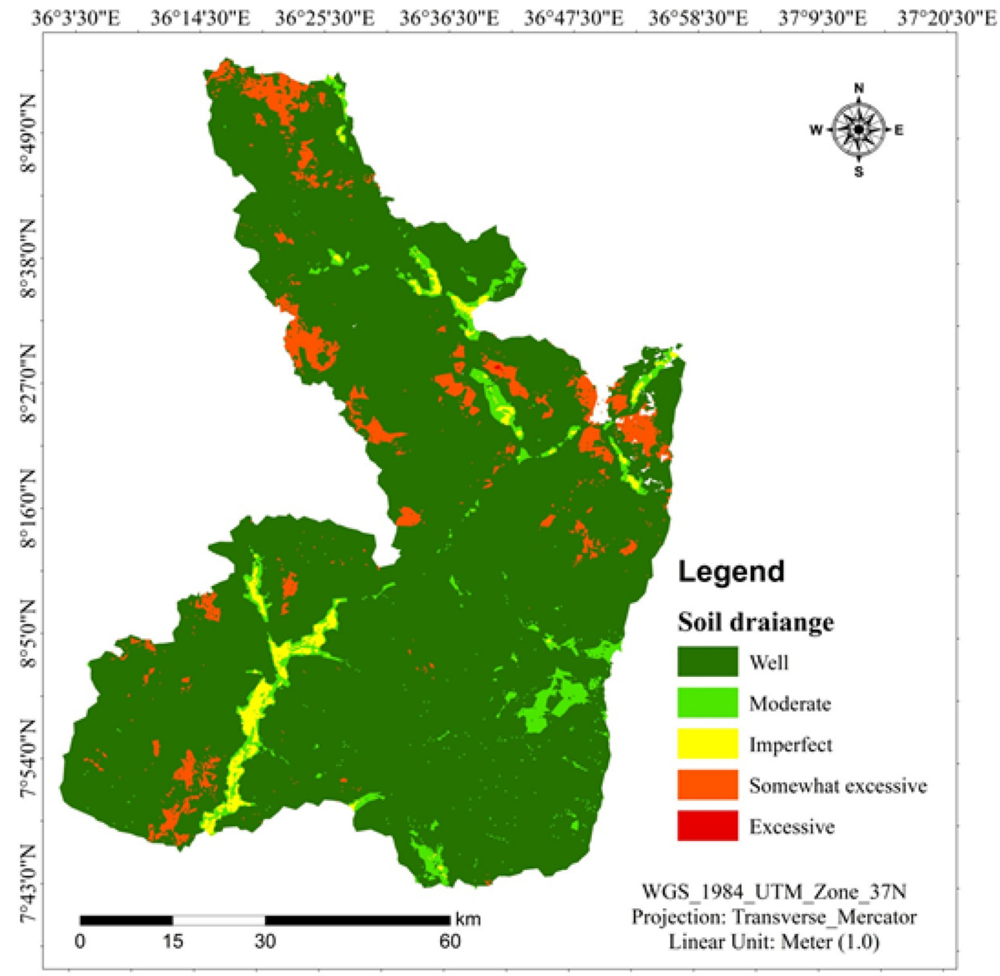

Fig. 8. Soil drainage map of the study area.

adequate (14.2%). This study's findings are consistent with earlier research (Sultan, 2013).

3.5. Soil texture

The study area's soil texture was divided into six groups. Sandy clay, clay loam, sandy clay loam, loam, sandy loam, and loamy sand. With an area of 80.7km^2 (1.2%) of the soil texture of the study area is highly appropriate for maize production. With a total area of 10.3km^2, sandy clay is unsuitable (0.8%). The sandy clay loam dominates most of the study region, which covers 3826.7km^2 (55.1%) and is moderately appropriate for maize agriculture (Table 6; Fig. 7). The study's findings were more consistent with those of the prior study (Hussien et al., 2019).

3.6. Soil drainage

Soil drainage map of the study area is presented (Fig. 8). There are five categories of drainage in the study area including well, moderate, somewhat excessive, excessive and imperfect. Study by Al-Mashreki et al. (2015) prove that well and moderate drainage were suitable for maize production. Results showed that 6143.1km^2 (88.5%) of the entire area of the Didessa watershed is highly suited for maize agriculture, whereas 372.7km^2 (5.4%) is not suitable (Table 7).

3.7. Soil depth

The most essential soil property for determining viable land for maize crop development is soil depth (Kindu et al., 2009). Maize crop productivity benefits greatly from deep soil depth. Based on soil depth we can classify land suitability for certain crops. The soil depth class of the study area is presented (Fig. 9). The results revealed that 4209.4km^2 (60.6%) is highly favorable for maize production, while 73.2km^2 (1.1%) is unsuitable (Table 8).

3.8. Land suitability for maize production

From aggregated eight factors, land suitability for maize production was produced (Fig. 10). The results showed that 977.7 km^2 (14.1%), and

Table 7
Soil drainage and suitability classes.

S/No	Soil drainage	Area (km^2)	Area (%)	Suitability classes
1	Imperfect	116.1	1.7	Marginally suitable
2	Moderate	311.0	4.5	Highly suitable
3	Well	6143.1	88.5	Not suitable
4	Somewhat excessive	372.0	5.4	Not suitable
5	Excessive	0.7	0.0	
	Total	6942.9	100.0	

Table 8
Soil depth and suitability classes.

S/No	Soil depth (cm)	Area (km^2)	Area (%)	Suitability classes
1	<50	73.2	1.1	Not suitable
2	50–75	778.2	11.2	Marginally suitable
3	75–100	1882.2	27.1	Moderately suitable
4	>100	4209.4	60.6	Highly suitable
	Total	6942.9	100.0	

4794.9 km^2 (69.1%), were highly, and moderately suitable for maize production, respectively while 1118.8 km^2 (16.1%), and 51.5 km^2 (0.7%) were marginally and not suitable for marginally and not suitable for maize production, respectively (Table 9). This data clearly indicates that majority of the study area is moderately suitable for maize production. Similar research findings were reported by Debesa et al. (2020) at Dabo Hana district. The lowland area, which is concentrated in the central part of the study area were highly and moderately suitable due to warm temperature (High LST) is more favorable for maize production. Consequently, western part and some eastern parts were

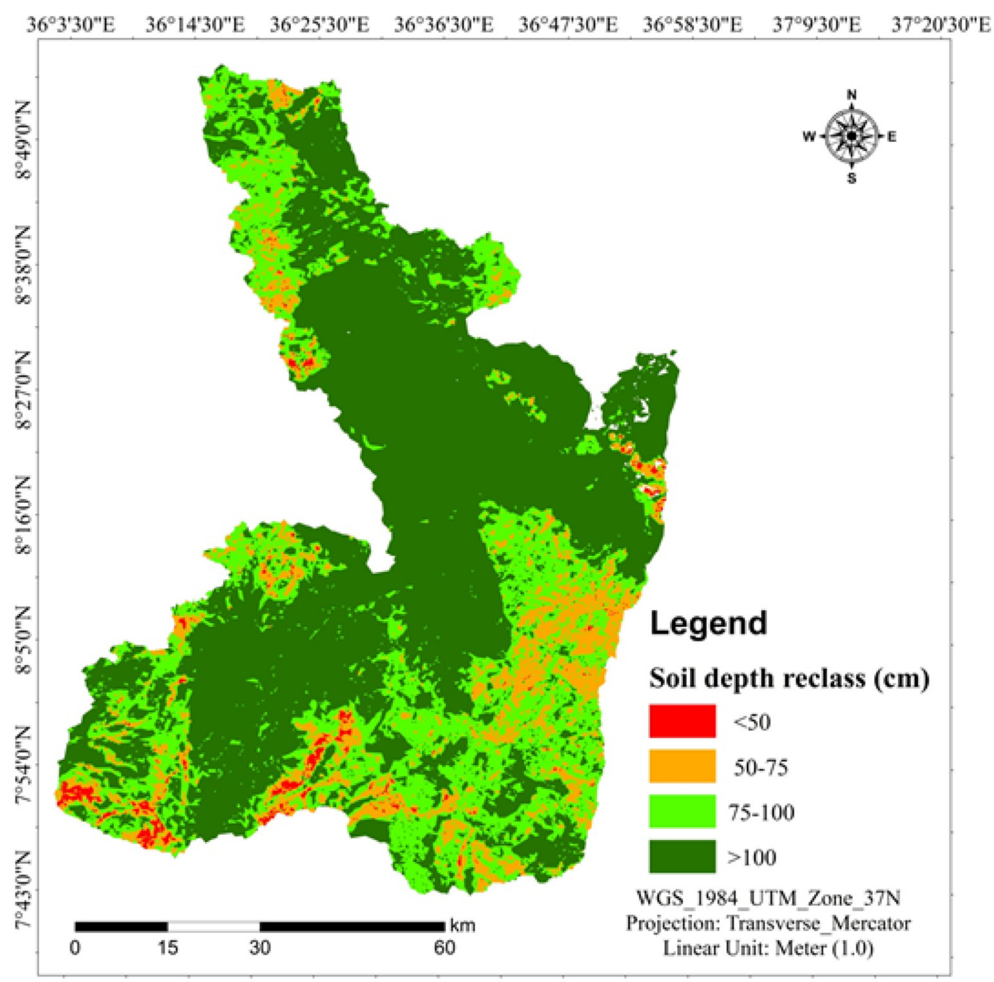

Fig. 9. Soil depth map of the study area.

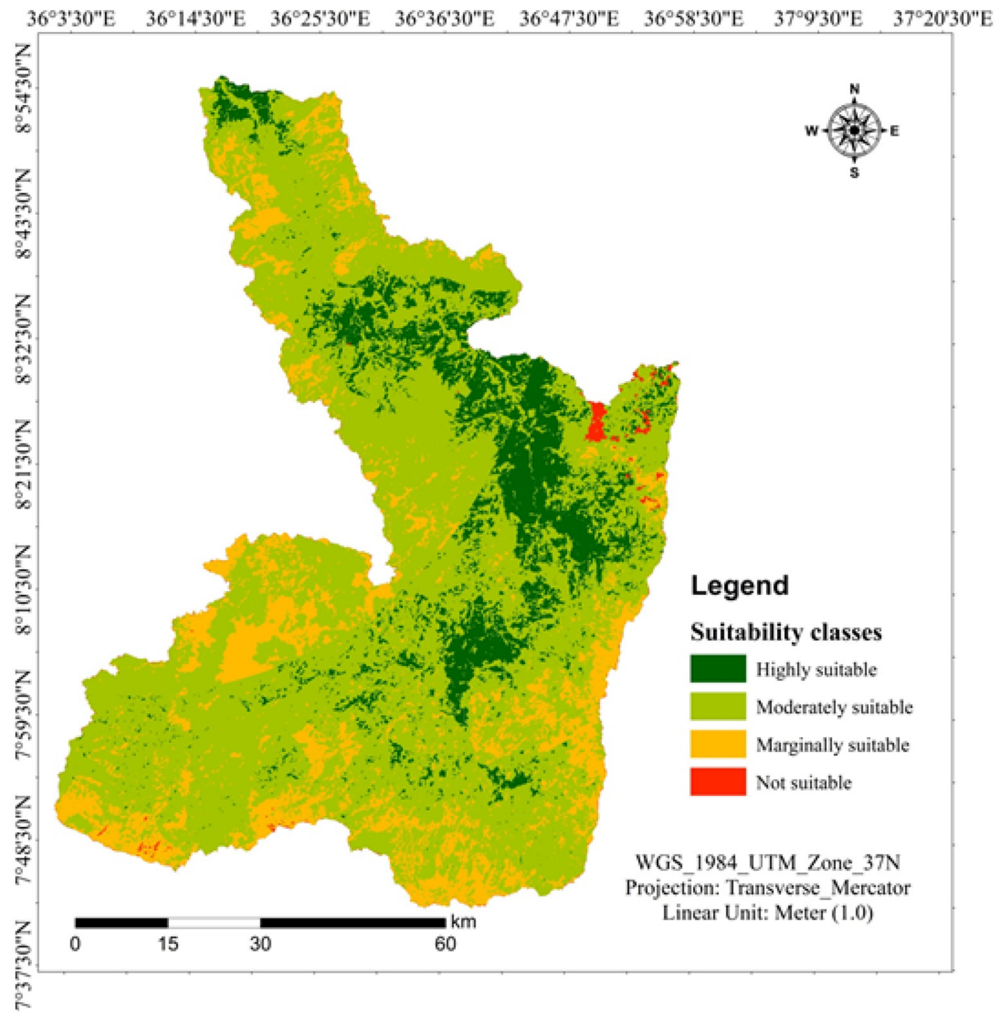

Fig. 10. Land suitability areas for maize production.

Table 9
Suitability area area for maize production.

S/No	Suitability classes	Area (km^2)	Area (%)
1	Highly suitable	977.7	14.1
2	Moderately suitable	4794.9	69.1
3	Marginally suitable	1118.8	16.1
4	Not suitable	51.5	0.7
	Total	6942.9	100.0

marginally suitable for maize production. Moreover, northeastern parts where elevated area and low temperatures were not suitable for maize production.

4. Conclusion

Understanding land suitability for crop production enhances yields and contributes towards the achievements of UN Sustainable Development Goals such as no poverty and zero hunger. Land suitability evaluation for maize production at watershed scale is crucial to enhance food security in agriculture-based economy like Ethiopia. Several factors such as: climate, LULC, LST, soil, topography, and infrastructure's data were used to evaluate physical land suitability for maize production. In this study, geospatial techniques were employed to identify physical land suitability for maize production in the study area. The results of the study showed that the area with low elevation and high LST are highly suitable for maize production. Results revealed that about 977.7km^2 (14.1%), and 4794.9km^2 (69.1%) were highly and moderately suitable for maize production, respectively. About 1118.8 km^2 (16.1%), and 51.5 km^2 (0.7%) were marginally and not suitable for maize production, respectively. The findings of this research can support decision making organs to promote intensive maize production in Didessa watershed. In order to enhance food security, the farming communities in the study area should cultivated the highly and moderately suitable area for maize production. Moreover, in order to sustain the life of the farming communities' similar crop specific physical land suitability will be conducted in the study area.

Compliance with ethical standards

NA.

Consent for publication

NA.

Availability of data

Data used for this study will be available based on request from the corresponding author.

Funding

No funding received for this research.

Credit authorship contribution statement

Mitiku Badasa Moisa: Conceptualization, Data curation, Formal analysis, Investigation, Methodology, Resources, Software, Validation, Visualization, Writing – original draft, Writing – review & editing. **Firdissa Sadeta Tiye:** Formal analysis, Investigation, Methodology, Resources, Writing – review & editing. **Indale Niguse Dejene:** Formal analysis, Investigation, Methodology, Resources, Writing – review & editing. **Dessalegn Obsi Gemeda:** Formal analysis, Investigation, Methodology, Resources, Writing – review & editing.

Declaration of Competing Interest

The authors declared no conflict of interests.

Acknowledgments

The authors acknowledge Wollega University Faculty of Technology, Shambu campus, Wollega University Gimbi campus, Wollega University Nekemte campus and Jimma University College of Agriculture and Veterinary Medicine for the existing facilities to conduct this research.

References

Abate, T., Shiferaw, B., Menkir, A., Wegary, D., Kebede, Y., Tesfaye, K., Kassie, M., Bogale, G., Tadesse, T., 2015. Factors that transformed maize productivity in Ethiopia. Food Security. 7, 965–981.

Abate, T.M., Dessie, A.B., Mekie, T.M., 2019. Technical efficiency of smallholder farmers in red pepper production in North Gondar zone Amhara regional state, Ethiopia. J. Econom. Struct. 8 (1), 1–18.

Abine, R.E., 2021. GIS and remote sensing assessment of landslide susceptibility along the Cameroon volcanic line: west region. Cameroon. Res. Square Platform LLC 2021. https://doi.org/10.21203/rs.3.rs-819468/v1.

Adeola, A.M., Olwoch, J.M., Botai, J.O., de Rautenbach, W.C.J., Kalumba, A.M., Tsela, P.L., Adisa, O.M., Nsubuga, F.W.N., 2017. Landsat satellite derived environmental metric for mapping mosquitoes breeding habitats in the Nkomazi municipality, Mpumalanga Province, South Africa. S. Afr. Geogr. J. 99 (1), 14–28.

Ahamed, T., Noguchi, R., Takigawa, T., Tian, L., 2016. Bio Production Engineering: Automation and Precision Agronomics for Sustainable Agricultural Systems. 2nd ed. Nova Science Publishers, Inc., New York, USA.

Aik, D.H.J., Ismail, M.H., Muharam, F.M., 2020. Land use/land cover changes and the relationship with land surface temperature using Landsat and MODIS imageries in Cameron Highlands, Malaysia. Land. 9, 372. https://doi.org/10.3390/land9100372.

Alemu, G., Worku, K., 2017. GIS-based land-use suitability analysis for selected perennial crops in Gumay Woreda of Jimma zone, south West Ethiopia. Ethiop. J. Soc. Sci. Lang. Stud. 4 (1), 3–18.

Al-Mashreki, M.H., Atroosh, K.B., Muflahi, A.A., Obaid, N.A., Caoline, K., 2015. GIS-based assessment of land suitability for industrial crops (cotton, sesame and groundnut) in the Abyan Delta, Yemen. Am. J. Exp. Agric. 8 (6), 384–405.

Al-Taani, A., Al-hubsan, Y., Farhan, I., 2021. Land suitability evaluation for agricultural use using GIS and remote sensing techniques: the case study of Ma'an governorate, Jordan. Egypt. J. Remote Sens. Space Sci. 24 (1), 109–117.

Asfaw, S., Shiferaw, B., Simtowe, F., Lipper, L., 2012. Impact of modern agricultural technologies on smallholder welfare: evidence from Tanzania and Ethiopia. Food Policy 37 (3), 283–295.

Berhanu, K., Poulton, C., 2014. The political economy of agricultural extension policy in Ethiopia: economic growth and political control. Dev. Policy Rev. 32 (s2), s197–s213.

Bewket, W., 2007. Soil and water conservation intervention with conventional technologies in northwestern highlands of Ethiopia: acceptance and adoption by farmers. Land Use Policy 24 (2), 404–416.

Cheng, X., Wei, B., Chen, G., Song, C., 2015. Influence of park size and its surrounding urban landscape patterns on the park cooling effect. J. Urban Plan. Dev. 141 (3), A4014002.

Chibuike, E.M., Lbukun, A.O., Kunda, J.J., Abba, A., 2018. Assessment of green parks cooling effect on Abuja urban microclimate using Geopspatial techniques. Rem. Sens. Appl. Soc. Environ. 11 (11–21). https://doi.org/10.1016/j.rsase.2018.04.006.

Debesa, G., Gebre, S.L., Melese, A., Regassa, A., Teka, S., 2020. GIS and remote sensing-based physical land suitability analysis for major cereal crops in Dabo Hana district, South-West Ethiopia. Cogent Food Agric. 6 (1), 1780100.

Dendir, Z., Simane, B., 2019. Livelihood vulnerability to climate variability and change in different agroecological zones of Gurage administrative zone, Ethiopia. Progr. Disast. Sci. 3, 100035.

Dener, E., Alves, L., 2016. Seasonal and spatial variation of surface urban heat island intensity in a small urban agglomerate in Brazil. Climate. 4 (4), 61. https://doi.org/10.3390/cli4040061.

Elias, A., Nohmi, M., Yasunobu, K., Ishida, A., 2013. Effect of agricultural extension program on Smallholders' farm productivity: evidence from three peasant associations in the highlands of Ethiopia. J. Agric. Sci. 5 (8). https://doi.org/10.5539/jas.v5n8p163.

Gemeda, D.O., Korecha, D., Garedew, W., 2021. Evidences of climate change presences in the wettest parts of Southwest Ethiopia. Heliyon. 9, e08009. https://doi.org/10.1016/j.heliyon.2021.e08009.

Girma, R., Moges, A., Quraishi, S., 2015. GIS based physical land suitability evaluation for crop production in eastern Ethiopia: A case study in Jello watershed. Agrotechnology. 4, 139. https://doi.org/10.4172/2168-9881.1000139.

Gorfu, D., Ahmed, E., 2011. Crops and Agro-Ecological Zones of Ethiopia. Senior Researchers, Ethiopian Institute of Agricultural Research. https://prrp-ethiopia.wur.nl/index/component/phocadownload/category/8-%20crops%20and%20agro-ecological%20zones%20total%20-%20dereje%20gorfu2770.pdf?download=51:crops-and-agro-ecological-zones-total-dereje-gorfu (Accessed on January 20, 2022).

Guo, J., Ren, H., Zheng, Y., Lu, S., Dong, J., 2020. Evaluation of land surface temperature retrieval from Landsat 8/TIRS images before and after stray light correction using the SURFRAD dataset. Remote Sens. 12 (6), 1023.

Habibie, M.I., Noguchi, R., Shusuke, M., Ahamed, T., 2019. Land suitability analysis for maize production in Indonesia using satellite remote sensing and GIS-based multi criteria decision support system. GeoJournal. 86, 777–807.

Headey, D., Dereje, M., Taffesse, A.S., 2014. Land constraints and agricultural intensification in Ethiopia: A village-level analysis of high-potential areas. Food Policy 48, 129–141.

Huffnagel, H.P., 1961. Agriculture in Ethiopia. FAO, Rome.

Hurni, H., 1998. Soil Conservation Research Programme Ethiopia Research Report Agro-ecological Belts of Ethiopia. Centre for Development and Environment University of Bern, Switzerland in Association with the Ministry of Agriculture, Ethiopia.

Hussien, K., Woldu, G., Birhanu, S., 2019. A GIS-based multi-criteria land suitability analysis for surface irrigation along the Erer watershed, eastern Hararghe zone, Ethiopia. East Afr. J. Sci. 13 (2), 169–184.

Kassie, B.T., Asseng, S., Rotter, R.P., Hengsdijk, H., Ruane, A.C., Van Ittersum, M.K., 2015. Exploring climate change impacts and adaptation options for maize production in the central Rift Valley of Ethiopia using different climate change scenarios and crop models. Clim. Chang. 129 (1), 145–158.

Kindu, M., Kidanu, S., Chernet, T., 2009. GIS-Based Agricultural Land Suitability for Target Crops. EIAR. Technical Report https://doi.org/10.13140/RG.2.2.18047.30887.

Linda, A., Oluwatola, A., Opeyemi, T.A., 2015. Land suitability analysis for maize production in Egbeda local government area of Oyo state using GIS techniques. World Academy of Science, Engineering and Technology. Int. J. Environ. Ecol. Eng. 9 (3), 294–299.

Malczewski, J., 2000. GIS and Multicriteria Decision Analysis. John Wiley & Sons. Canada, USA.

Mehrjardi, R.T., Nabiollahi, K., Rasoli, L., Kerry, R., Scholten, T.H., 2020. Land suitability assessment and agricultural production sustainability using machine learning models. Agronomy. 10, 573. https://doi.org/10.3390/agronomy10040573.

Moisa, M.B., Merga, B.B., Gemeda, D.O., 2022. Multiple Indices-Based Assessment of Agricultural Drought: A Case Study in Gilgel Gibe Sub-Basin. Theor Appl Climatol, Southern Ethiopia https://doi.org/10.1007/s00704-022-03962-4.

Mota, A.A., Lachore, S.T., Handiso, Y.H., 2019. Assessment of food insecurity and its determinants in the rural households in Damot Gale Woreda, Wolaita zone, southern Ethiopia. Agric. Food Security. 8 (1), 1–11.

Nyagumbo, I., Mkuhlani, S., Pisa, C., Kamalongo, D., Dias, D., Mekuria, M., 2016. Maize yield effects of conservation agriculture based maize–legume cropping systems in contrasting agro-ecologies of Malawi and Mozambique. Nutr. Cycl. Agroecosyst. 105 (3), 275–290.

Rabia, A.H., Terribile, F., 2013. Introducing a new parametric concept for land suitability assessment. Int. J. Environ. Sci. Dev. 4 (1), 15–19.

Rashid, Z., Zaidi, P.H., Vinayan, M.T., Sharma, S.S., Setty, T.S., 2013. Downy mildew resistance in maize (*Zea mays* L.) across Peronosclerospora species in lowland tropical Asia. Crop Prot. 43, 183–191.

Regassa, N., Stoecker, B.J., 2012. Household food insecurity and hunger among households in Sidama district, southern Ethiopia. Public Health Nutr. 15 (7), 1276–1283.

Saaty, T.L., 1980. The Analytic Hierarchy Processes. McGraw-Hill International, New York, NY.

Saaty, T.L., 2004. Decision making the analytic hierarchy and network processes (AHP/ANP). J. Syst. Sci. Syst. Eng. 13 (1), 1–35.

Sekertekin, A., Bonafoni, S., 2020. Sensitivity analysis and validation of daytime and nighttime land surface temperature retrievals from Landsat 8 using different algorithms and emissivity models. Remote Sens. 12, 2776. https://doi.org/10.3390/rs12172776.

Silva, J.V., Reidsma, P., Baudron, F., Jalet, A.M., Tesfaye, K., van Ittersum, M.K., 2021. Wheat yield gaps across smallholder farming systems in Ethiopia. Agron. Sustain. Dev. 41 (1), 1–16.

Sime, G., Aune, J.B., 2018. Sustainability of improved crop varieties and agricultural practices: A case study in the central Rift Valley of Ethiopia. Agriculture. 8 (11). https://doi.org/10.3390/agriculture8110177.

Sobrino A, José, Jiménez-Muñoz C, Juan, Paolini, Leonardo, 2004. Land surfacetemperature retrieval from LANDSAT TM5. Remote Sensing of Environment Volume 90 (4), 434–440. https://doi.org/10.1016/j.rse.2004.02.003.

Solanki, R.L., Nagar, K.C., Agarwal, S.K., Swami, P., Indoria, D., 2020. Evaluation of yield performance of soybean [*Glycine max* (L.) Merrill] through cluster front line demonstrations. Int. J. Curr. Microbiol. App. Sci. 9 (4), 2020. https://doi.org/10.20546/ijcmas.2020.904.xx.

Sultan, D., 2013. Assessment of irrigation land suitability and development of map for the Fogera catchment using GIS, South Gondar. Asian J. Agric. Rural Dev. 3 (1), 7–17.

Tamene, L., Amede, T., Kihara, J., Tibebe, D., Schulz, S., 2017. A review of soil fertility management and crop response to fertilizer application in Ethiopia: Towards development of site-and context-specific fertilizer recommendation. International Center for Tropical Agriculture (CIAT), Addis Ababa, Ethiopia , p. 86 (CIAT Publication No.443) https://hdl.handle.net/10568/82996.

Tessema, I., Simane, B., 2019. Vulnerability analysis of smallholder farmers to climate variability and change: an agro-ecological system-based approach in the Fincha'a sub-basin of the upper Blue Nile Basin of Ethiopia. Ecol. Process. 8 (1), 1–18.

Tomar, V., Kumar, P., Rani, M., Gupta, G., Singh, J., 2013. A satellite-based biodiversity dynamics capability in tropical vegetation. Electron. J. Geotech. Eng. 18, 1171–1180.

Van Dijk, Michiel, Morley, Tomas, van Loon, Marloes, Reidsma, Pytrik, Tesfaye, Kindie, van Ittersum K, Martin, 2020. Reducing the maize yield gap in Ethiopia: Decomposition and policy simulation. Agricultural Systems 183, 102828. https://doi.org/10.1016/j.agsy.2020.102828.

Vasu, D., Srivastava, R., Patil, N.G., Tiwary, P., Chandran, P., Singh, S.K., 2018. Acomparative assessment of land suitability evaluation method for agricultural land use planning at village level. Land Use Policy 79, 146–163.

Wedajo, G.K., Muleta, M.K., Gessesse, B., Koriche, S.A., 2019. Spatiotemporal climate and vegetation greenness changes and their nexus for Dhidhessa River basin, Ethiopia. Environ. Syst. Res. 8 (1), 1–24.

Yohannes, Hamere, Soromessa, Teshome, 2018. Land suitability assessment for major crops by using GIS-based multi-criteria approach in Andit Tid watershed, Ethiopia. Cogent Food & Agriculture 4 (1), 1470481. https://doi.org/10.1080/23311932.2018.1470481.

Ziaul, S.K., Pal, S., 2018. Zing control of respiratory particulate matter on land surface temperature in local climatic zones of English bazar municipality and surroundings. Urban Clim. 24, 34–50. https://doi.org/10.1016/j.uclim.2018.01.006.